

Parsimonious Modelling with Information Filtering Networks

Wolfram Barfuss^{1*}, Guido Previde Massara², T. Di Matteo^{2,3} and Tomaso Aste^{2,4}

¹ *Department of Physics, FAU Erlangen-Nürnberg, Nögelsbachstr. 49b, 91052 Erlangen, GER*

² *Department of Computer Science, University College London, Gower Street, London, WC1E 6BT, UK*

³ *Department of Mathematics, King's College London, The Strand, London, WC2R 2LS, UK*

⁴ *Systemic Risk Centre, London School of Economics and Political Sciences, London, WC2A2AE, UK*

**now at: Potsdam Institute for Climate Impact Research, Telegrafenberg A31, 14473 Potsdam, GER
and Department of Physics, Humboldt University, Newtonstr. 15, 12489 Berlin, GER*

(Dated: March 20, 2022)

We introduce a methodology to construct sparse models from data by using information filtering networks. This method estimates the global sparse inverse covariance from a simple sum of local inverse covariances computed on small sub-parts of the network. Being based on local, low-dimensional, inversions this method is computationally very efficient and statistically robust even for the estimation of inverse covariance of high-dimensional, noisy and short time-series. Compared with state-of-the-art methodologies such as Glasso, our method is computationally more efficient producing, in a fraction of the computation time, models that have equivalent or better performances but with a sparser and more meaningful inference structure. The local nature of this approach allows to preform computations in parallel and provides a tool for dynamical adaptation by partial updating when the properties of some variables change without the need of recomputing the whole model. This makes this approach particularly suitable to handle big datasets with a large number of variables. We discuss performances with financial data and financial applications to prediction, stress testing and risk allocation.

Keywords: complex systems, econophysics, information filtering, sparse inverse covariance, probabilistic modelling, graphical modelling, Glasso

I. INTRODUCTION

This paper addresses the following question: how can one construct, from a set of observations, the model that most meaningfully describes the underlying system? This is a general question that often arises in science and it is the core of so-called data-driven modelling. In the context of the present paper the ‘model’ is the multivariate probability distribution that best describes the set of observations. The problem of finding such a distribution becomes particularly challenging when the number of variables, p , is large and the number of observations, q , is small. Indeed, in such a multivariate problem, the model must take into account at least an order $O(p^2)$ of interrelations between the variables and therefore the number of model-parameters scales at least quadratically with the number of variables. A parsimonious approach requires to discover the model that best reproduces the statistical properties of the observations while keeping the number of parameters as small as possible. Using a maximum entropy approach up to the second order in the moments of the distribution, the model becomes the multivariate normal distribution. In the multivariate normal case there is a simple relationship between the sparsity pattern of the inverse of the covariance matrix (the precision matrix, henceforth denoted by \mathbf{J}) and the underlying partial correlation structure (referred to as graphical model in the literature [1]): two nodes i and j are linked in the graphical model if and only if the corresponding precision matrix element J_{ij} is different from zero. Therefore the problem of estimating a sparse precision matrix is equivalent to the problem of learning a sparse multivariate normal graphical model (known in the literature as Gaussian Markov Random Field (GMRF) [2]). Once the sparse precision matrix has been estimated, a number of efficient tools – mostly based on research in sparse numerical linear algebra – can be used to sample from the distribution, calculate conditional probabilities, calculate conditional statistics and forecast [2, 3]. GMRFs are of great importance in many applications spanning computer vision [4], sparse sensing [5], finance [6–10], gene expression [11–13]; biological neural networks [14], climate networks [15, 16]; geostatistics and spatial statistics [17–19]. Almost universally, applications require modelling a large number of variables with a relatively small number of observations and therefore the issue of the statistical significance of the model parameters is very important.

The problem of finding meaningful and parsimonious models, sometimes referred as sparse structure learning [20], has been tackled by using a number of different approaches. Let us hereafter briefly account for some of the most relevant in the present context.

Constraint based approaches recover the structure of the network by testing the local Markov property. Usually the algorithm starts from a complete model and adopts a *backward selection* approach by testing the independence of nodes conditioned on subsets of the remaining nodes (algorithms SGS and PC [20]) and removing edges associated to nodes that are conditionally independent; the algorithm stops when some criteria are met – e.g. every node has less

than a given number of neighbours. Conversely *forward selection* algorithms start from a sparse model and add edges associated to nodes that are discovered to be conditionally dependent. An hybrid model is the GS algorithm where a number of candidate edges is added to the model (the “grow” step) in a forward selection phase and subsequently reduced using a backward selection step (the “shrinkage” step) [20]. The complexity of checking a large number of conditional independence statements makes these methods unsuitable for moderately large graphs. Furthermore, aside from the complexity of measuring conditional independence, these methods do not generally optimize a global function, such as likelihood or the Akaike Information Criterion [21, 22] but they rather try to exhaustively test all the (local) conditional independence properties of a set of data and therefore are difficult to use in a probabilistic framework.

Score based approaches learn the structure trying to optimize some global function: likelihood, Kullback-Leibler divergence [23], Bayesian Information Criterion (BIC) [24], Minimum Description Length [25] or the likelihood ratio test statistics [26]. In these approaches, the main issue is that the optimization is generally computationally demanding and some sort of greedy approach is required.

In the field of *decomposable models* there are a number of methods that efficiently explore the graphical structure (directed, in the case of Bayesian models, or undirected in the case of log-linear or multivariate Gaussian models) by using advanced graph structures such as junction tree or clique graph [26–28], with the goal of producing sparse models (so-called “thin junction trees” [29–31]).

Other approaches [32–34] treat the problem as a constrained optimization problem to recover the sparse covariance matrix. Within this line, *regression based approaches* generally try to minimize some loss function which enforces parsimony and sparsity by using penalization to constrain the number and size of the regression parameters. Specifically ridge regression uses a ℓ_2 -norm penalty; instead the *lasso* method [35] uses an ℓ_1 -norm penalty and the elastic-net approach uses a convex combination of ℓ_2 and ℓ_1 penalties on the regression coefficients [36]. These approaches are among the best performing regularization methodologies presently available. The ℓ_1 -norm penalty term favours solutions with parameters with zero value leading to models with sparse inverse covariances. Sparsity is controlled by regularization parameters $\lambda_{ij} > 0$; the larger the value of the parameters the more sparse the solution becomes. This approach has become extremely popular and around the original idea a large body of literature has been published with several novel algorithmic techniques that are continuously advancing this method [35, 37–41] among these the popular implementation Glasso (Graphical-lasso) [42] which uses lasso to compute sparse graphical models. However, Glasso methods are computationally intensive and, although they are sparse, the non-zero parameters interaction structure tends to be noisy and not significantly related with the true underlying interactions between the variables.

It has been proven in several applications that information filtering networks such as Maximum Spanning Tree (MST) or Planar Maximally Filtered Graphs (PMFG) from correlation matrices are powerful tools to extract the relevant interaction structure from multivariate datasets [6–8, 43–45]. A new family of information filtering networks, the triangulated maximal planar graph (TMFG) [46], was recently introduced. These are planar graphs, similar to the PMFG, but with the advantages to be generated in a computationally efficient way and, more importantly for this paper, they are decomposable graphs (see example in Fig.1). A decomposable graph has the property that every cycle of length greater than three has a chord, an edge that connect two vertices of the cycle in a smaller cycle of length three. Decomposable graphs, also called chordal or triangulated, are clique trees, made of k -cliques (complete sub graphs of k vertices) connected by separators. Separators are also cliques of smaller sizes with the property that the graph becomes divided into two or more disconnected components when the vertices of the separator are disconnected. In the schematic representation of the TMFG reported in Fig.1 the cliques are the tetrahedra $\{1, 2, 3, 4\}$ and $\{2, 3, 4, 5\}$ whereas the separator is the triangle $\{2, 3, 4\}$.

The novelty of the method presented in this paper is the combination of decomposable information filtering networks [6–10] with Gaussian Markov Random Fields [1, 2] to produce parsimonious models associated with a meaningful structure of dependency between the variables. The strength of this methodology is that the global sparse inverse covariance matrix is produced from a simple sum of local inversions. This makes the method computationally very efficient and statistically highly robust. Given the Local/Global nature of its construction in the following we shall refer to this method as LoGo. In this paper, we demonstrate that the structure provided by information filtering networks is also extremely effective to generate high-likelihood sparse models. The LoGo sparse inverse covariance has only $O(p)$ parameters but, despite its sparsity, the associated multivariate normal distribution can still retrieve high likelihood values yielding comparable or better results than state-of-the-art Glasso penalized inversions.

The rest of the paper is organized as follows: In Section II we describe our methodology providing algorithms for sparse covariance inversion for two graph topologies: the maximum spanning tree (MST) and the TMFG. We then show in Section III that our method yields comparable or better results in maximum likelihood compared to lasso-type and ridge regression estimates of the inverse covariances. Subsequently we discuss how our approach can be used in time series prediction, financial stress testing and risk allocation. With Section IV we end with possible extensions for future work and conclusive remarks.

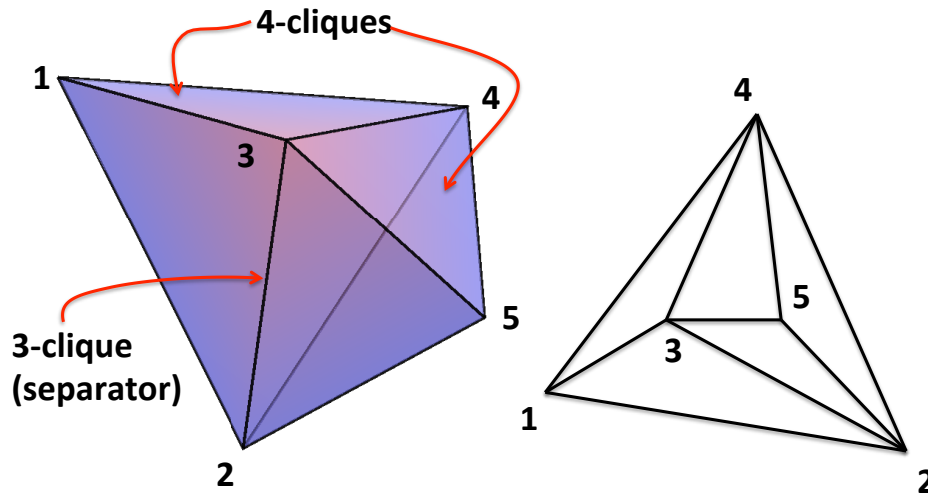


FIG. 1: **Two schematic representations of a TMFG network.** The network is made of two cliques of four nodes (4-cliques) and one separator of three nodes (3-clique). The cliques are the tetrahedra $\{1, 2, 3, 4\}$ and $\{2, 3, 4, 5\}$ and the separator is the triangle $\{2, 3, 4\}$. This is a chordal graph.

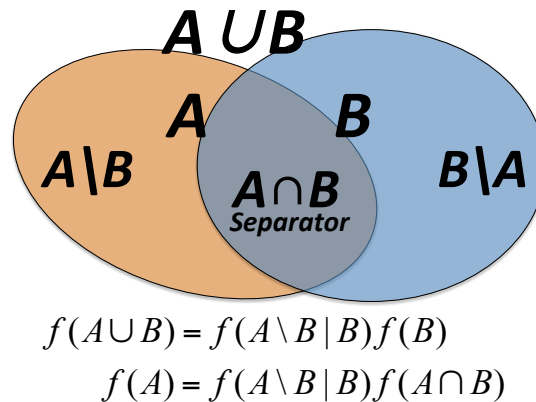


FIG. 2: **Decomposition of the joint probability distribution function.** Bayes formulas for two sets of variables A and B with a separating set $A \cap B$. Variables within sets A or B are assumed conditionally dependent whereas variables belonging to the two separated sets $A \setminus B$ and $B \setminus A$ are assumed independent conditionally to $A \cap B$. By combining the two formulas one obtains: $f(A \cup B) = f(A) f(B) / f(A \cap B)$.

II. PARSIMONIOUS MODELLING WITH INFORMATION FILTERING NETWORKS

A. Factorization of the multivariate probability distribution function

Let us start by demonstrating how a decomposable information filtering network can be associated with a convenient factorization of the multivariate probability distribution. Let us consider, in general, two sets A and B of variables with non empty intersection $A \cap B \neq \emptyset$. Let us also assume that the variables are mutually dependent within the same ensemble A or B but when one variable belongs to set $A \setminus B$ and the other variable belongs to set $B \setminus A$, then they are independent conditioned to $A \cap B$. We can now use the Bayes formula: $f(A \cup B) = f(A \setminus B | B) f(B)$ where $f(A \cup B)$ is the joint probability distribution function of all variable in A and B , $f(A \setminus B | B)$ is the conditional probability distribution function for the variables in A minus the subset in common with B conditioned to all variables in B and $f(B)$ is the marginal probability distribution function of all variables in B (see Fig.2). From the Bayes formula we also have the following identity: $f(A) = f(A \setminus B | B) f(A \cap B)$ that combined with the previous gives the following

factorization for the joint probability distribution function of all variable in A and B [1]:

$$f(A \cup B) = \frac{f(A)f(B)}{f(A \cap B)} \quad (1)$$

Let us now apply this formula to a set of variables associated with a decomposable information filtering network \mathcal{G} made of M cliques, \mathcal{C}_m , with $m = 1, \dots, M$ and $M - 1$, possibly repeated, separators \mathcal{S}_n , with $n = 1, \dots, M - 1$. In such a network, the vertices are representing the p variables X_1, \dots, X_p and the edges are representing couples of conditionally dependent variables (condition being with respect to all another variables). Conversely variables which are not directly connected with a network edge are conditionally independent. Given such a network, in the same way as for Eq.1, one can write the joint probability density function for the set of p variables $\mathbf{X} = (X_1, X_2, \dots, X_p)^\top$ in terms of the following factorization into cliques and separators [1]:

$$f(\mathbf{X}) = \frac{\prod_{m=1}^M f_{\mathcal{C}_m}(\mathbf{X}_{\mathcal{C}_m})}{\prod_{n=1}^{M-1} f_{\mathcal{S}_n}(\mathbf{X}_{\mathcal{S}_n})^{k(\mathcal{S}_n)-1}} \quad (2)$$

where $f_{\mathcal{C}_m}(\mathbf{X}_{\mathcal{C}_m})$ and $f_{\mathcal{S}_n}(\mathbf{X}_{\mathcal{S}_n})$ are respectively the marginal probability density functions of the variables constituting \mathcal{C}_m and \mathcal{S}_n [1]. The term $k(\mathcal{S}_n)$ counts the number of disconnected components produced by removing the separator \mathcal{S}_n and it is therefore the degree of the separator in the clique tree. Given the graph \mathcal{G} , Eq.2 is exact, it is a direct consequence of the Bayes formula and it is therefore very general.

B. Functional form of the multivariate probability distribution function

We search for the functional form of the multivariate probability distribution function, $f(\mathbf{X})$. To find the functional form of the distribution f and the values of its parameters \mathbf{J} , we use the maximum entropy method [47, 48] which constrains the model to have some given expectation values while maximising the overall information entropy $-\int f(\mathbf{X}) \log f(\mathbf{X}) d^p \mathbf{X}$. At the second order, the model distribution that maximizes entropy while constraining moments at given values is:

$$f(\mathbf{X}) = \frac{1}{Z} \exp \left(- \sum_{ij} \frac{1}{2} (X_i - \mu_i) J_{i,j} (X_j - \mu_j) \right) ; \quad (3)$$

where $\boldsymbol{\mu} \in \mathbb{R}^{p \times 1}$ is the vector of expectation values with coefficients $\mu_i = \mathbb{E}[X_i]$ and $J_{i,j}$ are the matrix elements of $\mathbf{J} \in \mathbb{R}^{p \times p}$. They are the Lagrange multipliers associated with the second moments of the distribution $\mathbb{E}[(X_i - \mu_i)(X_j - \mu_j)] = \Sigma_{i,j}$ which are the coefficients of the covariance matrix $\boldsymbol{\Sigma} \in \mathbb{R}^{p \times p}$. It is clear that Eq.3 is a multivariate normal distribution with $Z = \sqrt{(2\pi)^p \det(\boldsymbol{\Sigma})}$. If we require the model $f(\mathbf{X})$ to reproduce exactly all second moments $\Sigma_{i,j}$, then the solution is $\mathbf{J} = \boldsymbol{\Sigma}^{-1}$. Therefore, in order to construct the model, one could estimate empirically the covariance matrix $\hat{\boldsymbol{\Sigma}}$ from a set of q observations and then invert it in order to estimate the inverse covariance. However, in the case when the observation length q is smaller than the number of variables p the empirical estimate of the covariance matrix $\hat{\boldsymbol{\Sigma}}$ cannot be inverted. Furthermore, also in the case when $q > p$, such a model has $p(p+3)/2$ parameters and this might be an overfitting solution describing noise instead of the underlying relationships between the variables resulting in poor predictive power [12, 49]. Indeed, we shall see in the following that, when uncertainty is large (q small), models with a smaller number of parameters can have stronger predictive power and can better describe the statistical variability of the data [50]. Here, we consider a parsimonious modelling that fixes only a selected number of second moments and leaves the others unconstrained. This corresponds to model the multivariate distribution by using a *sparse inverse covariance* where the unconstrained moments are associated with zero coefficients in the inverse. Let us note that this in turns implies zero partial correlation between the corresponding couples of variables.

C. Sparse inverse covariance from decomposable information filtering networks

From Eq.2 it follows that, in the case of the multivariate normal distribution, the network \mathcal{G} coincides with the structure of non-zero coefficients, $J_{i,j}$ in Eq.3 and their values can be computed from the local inversions of the covariance matrices respectively associated with the cliques and separators [1]:

$$J_{i,j} = \sum_{\mathcal{C} \text{ s.t. } \{i,j\} \in \mathcal{C}} (\boldsymbol{\Sigma}_{\mathcal{C}}^{-1})_{i,j} - \sum_{\mathcal{S} \text{ s.t. } \{i,j\} \in \mathcal{S}} (k(\mathcal{S}) - 1) (\boldsymbol{\Sigma}_{\mathcal{S}}^{-1})_{i,j} \quad (4)$$

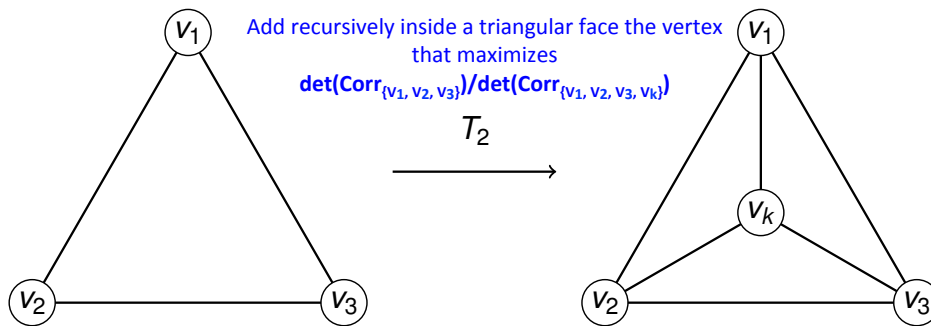


FIG. 4: **TMFG construction.** The TMFG graph is generated by adding vertices (e.g. v_k) inside triangular faces (e.g. $\{v_1, v_2, v_3\}$) maximising the ratio of the determinants between separator and clique $\det(\hat{\mathbf{R}}_{\{v_1, v_2, v_3\}})/\det(\hat{\mathbf{R}}_{\{v_1, v_2, v_3, v_k\}})$. This move generates a new 4-clique $\mathcal{C} = \{v_1, v_2, v_3, v_k\}$ and transforms the triangular face into a separator $\mathcal{S} = \{v_1, v_2, v_3\}$.

local inversion, Eq.4, on the MST structure. Note that the MST structure depends only on the correlations not the covariance.

The LoGo-TMFG construction requires a specifically designed procedure. Also in this case, only correlations matter; indeed, the structure of the inverse covariance network reflects the partial correlations i.e. the correlation between two variables given all others. TMFG starts with a tetrahedron, $\mathcal{C}_1 = \{v_1, v_2, v_3, v_4\}$, with smallest correlation determinant $\det \hat{\mathbf{R}}_{\mathcal{C}_1}$ and then iteratively introduces inside existing triangular faces the vertex that maximizes $\log \det \hat{\mathbf{R}}_{\mathcal{S}} - \log \det \hat{\mathbf{R}}_{\mathcal{C}}$ where \mathcal{C} and \mathcal{S} are the new clique and separator created by the vertex insertion. The LoGo-TMFG procedure is schematically reported in Algorithm 1 and in Fig. 4. The TMFG is a computationally efficient algorithm [46] that produces a decomposable (chordal) graph, with $3(p-2)$ edges, which is a clique-tree constituted by four-cliques connected with three-cliques separators. Note that for TMFG $k(\mathcal{S}_n) = 2$ always.

input : A covariance matrix $\hat{\Sigma} \in \mathbb{R}^{p \times p}$ and associated correlation matrix $\hat{\mathbf{R}} \in \mathbb{R}^{p \times p}$ from a set of observations $\{x_{1,1}, \dots, x_{1,q}\}, \{x_{2,1}, \dots, x_{2,q}\}, \dots, \{x_{p,1}, \dots, x_{p,q}\}$
output: **J** a sparse estimation of Σ^{-1}

- 1 **J** \leftarrow **0** Initialize **J** with zero elements;
- 2 $\mathcal{C}_1 \leftarrow$ Tetrahedron, $\{v_1, v_2, v_3, v_4\}$, with smallest $\det \hat{\mathbf{R}}_{\mathcal{C}_1}$;
- 3 $\mathcal{T} \leftarrow$ Assign to \mathcal{T} the four triangular faces in \mathcal{C}_1 : $\{v_1, v_2, v_3\}, \{v_1, v_2, v_4\}, \{v_1, v_4, v_3\}, \{v_4, v_2, v_3\}$;
- 4 $\mathcal{V} \leftarrow$ Assign to \mathcal{V} the remaining $p-4$ vertices not in \mathcal{C}_1 ;
- 5 **while** \mathcal{V} is not empty **do**
- 6 find the combination of $\{v_a, v_b, v_c\} \in \mathcal{T}$ and $v_d \in \mathcal{V}$ with largest $\det(\hat{\mathbf{R}}_{\{v_a, v_b, v_c\}})/\det(\hat{\mathbf{R}}_{\{v_a, v_b, v_c, v_d\}})$;
 // $\{v_a, v_b, v_c, v_d\}$ is a new 4-clique \mathcal{C} , $\{v_a, v_b, v_c\}$ becomes a separator \mathcal{S} , three new triangular faces,
 $\{v_a, v_b, v_d\}, \{v_a, v_c, v_d\}$ and $\{v_b, v_c, v_d\}$ are created
- 7 Remove v_d from \mathcal{V} ;
- 8 Remove $\{v_a, v_b, v_c\}$ from \mathcal{T} ;
- 9 Add $\{v_a, v_b, v_d\}, \{v_a, v_c, v_d\}, \{v_b, v_c, v_d\}$ to \mathcal{T} ;
- 10 Compute $J_{i,j} = J_{i,j} + \left(\Sigma_{\{v_a, v_b, v_c, v_d\}}^{-1}\right)_{i,j} - \left(\Sigma_{\{v_a, v_b, v_c\}}^{-1}\right)_{i,j}$;
- 11 **end**
- 12 **return J**;

Algorithm 1: LoGo-TMFG algorithm. The non-zero elements of **J** are the edges of \mathcal{G} which is a chordal graph, a clique tree, made of tetrahedra separated by triangles.

Let us note that by expanding to the second order in the correlation coefficients, the logarithms of the determinants become equal to a constant minus the sum of the square correlation coefficients associated with the edges in the cliques or separators. This can simplify the algorithm and the TMFG could be simply computed from a set of weight given by the squared correlation coefficients matrix, as described in [46].

Further, let us note that, for simplicity, in this paper we only consider likelihood maximization. A natural, straightforward extension of the present work is to consider Akaike Information Criterion [21, 22] instead. However, we have verified that, for the cases studied in this paper the two approaches give very similar results.

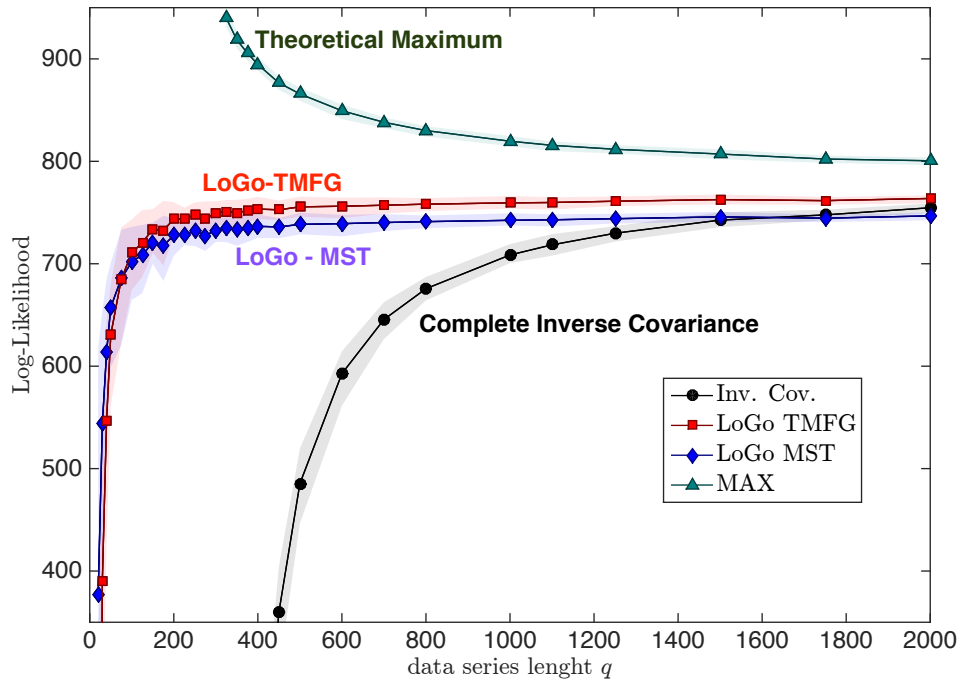


FIG. 5: **Demonstration that LoGo sparse inverse covariance represents the dependency structure better than the complete inverse covariance.** The figure reports comparisons between log-likelihood for models constructed by using sparse inverse LoGo-TMFG, LoGo-MST and the complete inverse of the empirical covariance matrix (Inv. Cov.). The measures are on $p = 300$ off-sample test data-series of different lengths q varying from 20 to 2000. The inverse matrices are computed on training datasets of the same length. Data are log-returns sampled from 342 stocks prices of equities traded on the US market during the period 1997-2012. The statistics is made stationary by random shuffling the time order. Symbols correspond to averages over 100 samples generated by picking at random 300 series over the 342 and assigning training and testing sets by choosing at random two non-overlapping time-windows of length q , the shaded bands are the 95% quantiles. The line on the top, labelled with ‘MAX’, is the theoretical maximum log-likelihood obtained from the inverse covariance of the testing set.

III. RESULTS

A. Inverse covariance estimation

We investigated stock prices time series from a US equity market computing the daily log-returns ($x_i(t) = \log Price_i(t) - \log Price_i(t-1)$ with $i = 1, \dots, 342$ and $t = 1, \dots, T$ with $T = 4025$ days during a period of 15 years from 1997 to 2012 [9]). We build 100 different datasets by creating stationary time series of different lengths selecting returns at random points in time and randomly picking $p = 300$ series out of the 342 in total. Each dataset was divided into two temporal non-overlapping windows with q elements constituting the ‘training set’ and other q elements the ‘testing set’.

We computed the log likelihood of the testing dataset using the inverse covariance estimates from the training set. Figure 5 reports the result for time series of different lengths from $q = 25$ to $q = 2000$. Let us first note that the green upward triangles, denoted MAX, are the theoretical maximum from the inverse sample covariance matrix calculated on the testing set which is reported to indicate the upper value for the attainable likelihood. We see from the figure that LoGo-TMFG outperforms the likelihood from the inverse covariance solution $\mathbf{J} = \hat{\Sigma}^{-1}$ (Inv. Cov.). For $q < p = 300$ the inverse covariance is not computable and therefore comparison cannot be made; when $q > p = 300$, the inverse covariance is computable but it performs very poorly for small sample sizes $q \sim p$ becoming comparable to LoGo-TMFG only after $q \sim 1500$ with both approaching the theoretical maxima at $q \rightarrow \infty$. Note that also LoGo-MST outperforms the inverse covariance solution in most of the range of q .

We compared the log-likelihood from LoGo-MST and LoGo-TMFG sparse inverse covariance with state-of-the-art Glasso ℓ_1 -norm penalized sparse inverse covariance models and Ridge ℓ_2 -norm penalized inverse model. Glasso method depends on the regularization parameters which were estimated by using two standard methods: i) G-Lasso-CV that used a two-fold cross validation method [55]; ii) G-Lasso-Sp which fixes the regularization parameter to the value that creates in the training set a sparse inverse with sparsity equal to LoGo-TMFG network ($3(p-2)$ parameters).

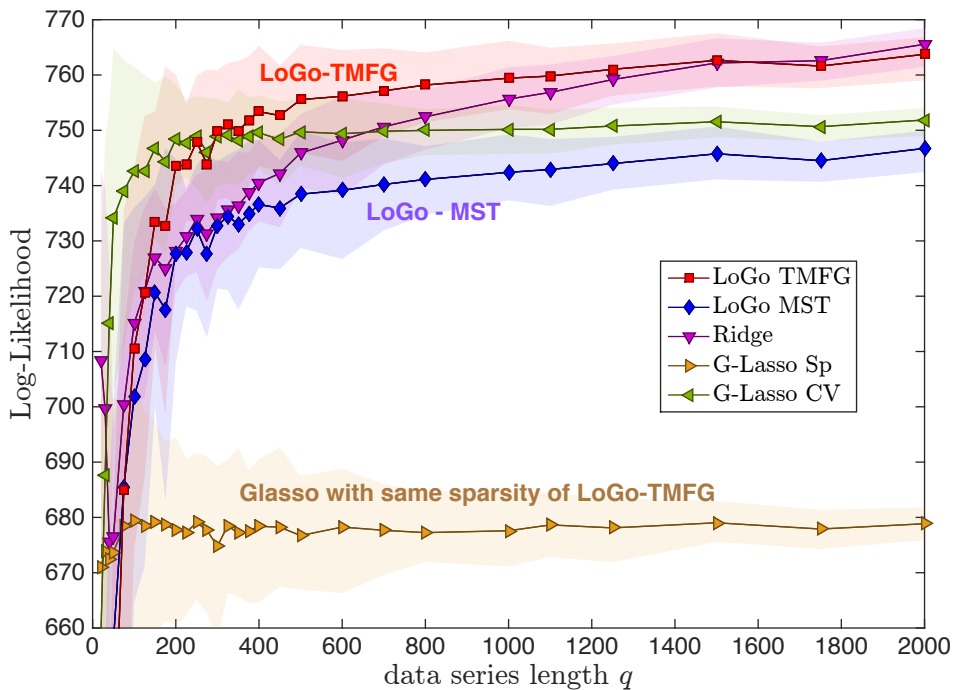


FIG. 6: **Demonstration that LoGo sparse modelling has better performances than Glasso with same sparsity.** This figure reports the same log-likelihood as in Fig.5 compared with log-likelihood from state-of-the-art Glasso ℓ_1 penalized sparse inverse covariance models (cross validated, G-Lasso-CV, and of the same sparsity of TMFG, G-Lasso-Sp) and Ridge ℓ_2 penalized inverse model (Ridge).

Ridge inverse penalization parameter was also computed by cross validation method [55]. Fig.6 reports a comparison between these methods for various values of q . We can observe that LoGo-TMFG outperforms the Glasso methods achieving larger likelihood from $q > 100$. Results are detailed in Table I.

The previous results are for time series made stationary by random selecting log-returns at different times. In practice, financial time series - and other real world signals - are non-stationary having statistical properties that change with time. Table II reports the same analysis as in Fig.6 and Table I but in temporal sequence with the training set being the q data points preceding the testing set. Let us note that, considering the time-period analysed, in the case of large q , the training set has most data points in the period preceding the 2007-2008 financial crisis whereas the testing set has data in the period following the crisis. Nonetheless, we see that the results are comparable with the one obtained for the stationary case. Surprisingly, we observe that for relatively small time-series lengths the values of the log-likelihood achieved by the various models is larger than in the stationary case. This counter-intuitive fact can be explained by the larger temporal persistence of real data with respect to the randomized series.

We also investigated artificial datasets of $p = 300$ multivariate variables generated from factor models respectively with 3 and 30 common factors. Results for the average log-likelihood and the standard deviations computed over 100 samples at different values of q are reported in Table III. Again we observe similar relative performances with LoGo performing consistently better than the inverse covariance, better than Glasso models of equal sparsity and comparably well with cross validated Glasso. Note that by increasing the number of factors performances of all models become worse.

B. Time series prediction

LoGo estimates the joint probability distribution function yielding the set of parameters for the model system's dependency structure. Here we demonstrate how this model can be used also for forecasting and to predict the future. Indeed, let us consider the set, \mathbf{X}_1 , of variables in the past and the set, \mathbf{X}_2 , of variables in the future. In general, we can consider to have p different variables and ℓ lags in the past yielding therefore a system of $p \times \ell$ variables in the past and p variables in the future. For simplicity of notation, and without loss of generality, we consider centred variables with zero expectation values. We can consider \mathbf{X}_1 and \mathbf{X}_2 as two distinct sets of variables that, of course, have some dependency relation. From a statistical perspective, prediction consists in estimating the expected values

TABLE I: **Demonstration that LoGo sparse modelling has better or comparable performances that state-of-the-art models.** Comparison between log-likelihood for LoGo, Glasso, Ridge, Complete inverse and Null models. Measures are on $p = 300$ off-sample test data-series of lengths $q = 50, 100, 300, 500, 1000, 2000$. Data are the same as in Fig.6: log-returns sampled from 342 stocks prices made stationary by random shuffling the time order in the time-series. The values reported are the averages of 100 samples and the standard deviations are reported between brackets. ‘MAX’, is the theoretical maximum log-likelihood obtained from the inverse covariance of the testing set.

q	50	100	300	500	1000	2000
Inv. Cov.	-	-	112 (53)	485 (29)	709 (8)	755 (4)
LoGo TMFG	631 (52)	711 (28)	753 (9)	756 (8)	759 (5)	764 (3)
LoGo MST	658 (43)	702 (28)	737 (9)	738 (8)	742 (5)	747 (3)
Ridge	676 (17)	715 (11)	741 (6)	746 (6)	756 (5)	766 (3)
G-Lasso Sp	674 (23)	679 (18)	678 (10)	677 (8)	678 (5)	679 (2)
G-Lasso CV	734 (25)	743 (15)	750 (5)	750 (5)	750 (4)	752 (2)
MAX	-	-	895 (6)	866 (5)	820 (4)	801 (3)
NULL	-276 (0.02)	-276 (0.02)	-276 (0.01)	-276 (0.01)	-276 (0.01)	-276 (0.00)

TABLE II: **LoGo performances on historic data.** Same analysis as in Table I performed for historic data where the training sets are past log-returns and the testing sets are future log-returns from two non-overlapping adjacent windows of length q .

q	50	100	300	500	1000	2000
Inv. Cov.	-	-	-	253 (835)	481 (335)	678 (15)
LoGo TMFG	679 (212)	757 (120)	674 (247)	665 (312)	605 (211)	694 (12)
LoGo MST	699 (202)	747 (120)	656 (255)	641 (324)	583 (221)	678 (11)
Ridge	753 (113)	746 (86)	721 (113)	721 (155)	684 (115)	710 (10)
G-Lasso Sp	722 (110)	704 (107)	664 (113)	627 (159)	625 (97)	659 (4)
G-Lasso CV	769 (134)	761 (89)	718 (110)	700 (178)	666 (120)	711 (6)
MAX	-	-	-	919 (63)	869 (40)	851 (3)
NULL	-276 (0.14)	-276 (0.07)	-276 (0.08)	-276 (0.07)	-276 (0.06)	-276 (0.00)

of the variables in the future given the values of the variables in the past. These expected values of the future variables are the conditional expectation values:

$$\boldsymbol{\mu}_{2|1} = \mathbb{E}[\mathbf{X}_2 | \mathbf{X}_1] . \quad (7)$$

These conditional expectation values can be calculated from the conditional joint distribution function, which, from the Bayes theorem, is $f(\mathbf{X}_2 | \mathbf{X}_1) = f(\mathbf{X}_2, \mathbf{X}_1) / f(\mathbf{X}_1)$. From this expression one obtains the following equation for the conditional expectation values:

$$\mathbf{J}_{2,2} \boldsymbol{\mu}_{2|1} = -\mathbf{J}_{2,1} \mathbf{X}_1 . \quad (8)$$

TABLE III: **LoGo performances on artificial data.** Same analysis as in Table I performed for artificial data generated with two factor models respectively with 3 (a) and 30 (b) factors.

(a)					(b)				
q	50	400	1000	2000	q	50	400	1000	2000
Inv. Cov.	-	-394 (14)	-63 (17)	-46 (18)	Inv. Cov.	-	-484 (12)	-143 (12)	-115 (11)
LoGo TMFG	-98 (13)	-51 (17)	-51 (18)	-58 (20)	LoGo TMFG	-440 (7)	-376 (2)	-373 (1)	-372 (2)
LoGo MST	-142 (10)	-116 (13)	-116 (11)	-121 (13)	LoGo MST	-432 (5)	-400 (3)	-393 (1)	-392 (1)
Ridge	-163 (8)	-82 (16)	-53 (15)	-48 (17)	Ridge	-324 (11)	-158 (9)	-129 (12)	-113 (11)
G-Lasso Sp	-452 (9)	-447 (4)	-447 (3)	-447 (2)	G-Lasso Sp	-430 (3)	-425 (1)	-424 (1)	-424 (1)
G-Lasso CV	-128 (7)	-62 (13)	-61 (11)	-55 (15)	G-Lasso CV	-326 (5)	-151 (6)	-130 (14)	-118 (11)
MAX	-	59 (18)	2 (17)	-20 (18)	MAX	-	-18 (9)	-78 (12)	-88 (11)
NULL	-427 (12)	-425 (6)	-426 (3)	-425 (2)	NULL	-425 (4)	-426 (1)	-425 (1)	-426 (1)

Where $\mathbf{J}_{2,2}$ is the $p \times p$ part of the precision matrix associated with the covariance of variables \mathbf{X}_2 and $\mathbf{J}_{2,1}$ is the $p \times (p \times \ell)$ part of the precision matrix associated with the cross-covariance of variables \mathbf{X}_2 and \mathbf{X}_1 . We must stress that Eq.8 is a different way to write the linear regression which, in a more conventional form, reads: $\mathbf{X}_2 = \beta \mathbf{X}_1 + \epsilon$ with the coefficients $\beta = -\mathbf{J}_{2,2}^{-1} \mathbf{J}_{2,1}$ and the residuals given by $\epsilon = \mathbf{X}_2 - \mu_{2|1}$. However, by using LoGo, Eq.8 becomes a sparse predictive model. Indeed, we can use LoGo to best estimate the joint probability distribution function $f(\mathbf{X}_2, \mathbf{X}_1)$ for the set of $p \times (\ell + 1)$ variables obtaining the associated sparse inverse covariance that is a block matrix:

$$\mathbf{J} = \begin{pmatrix} \mathbf{J}_{1,1} & \mathbf{J}_{1,2} \\ \mathbf{J}_{2,1} & \mathbf{J}_{2,2} \end{pmatrix} . \quad (9)$$

LoGo therefore can provide sparse estimates for the matrices $\mathbf{J}_{2,1}$ and $\mathbf{J}_{2,2}$ which substituted in Eq.8 give $\mu_{2|1}$. Note that Eq.8 is a map describing the impact of variables in the past onto the future; non-zero elements of $\mathbf{J}_{2,1}$ single out the variables that have future impact. The structure of $\mathbf{J}_{2,2}$ discloses instead systemic vulnerability. Indeed, the expected conditional fluctuations of the variables \mathbf{X}_2 are given by the conditional covariance:

$$\mathbf{Cov}(\mathbf{X}_2 | \mathbf{X}_1) = \mathbf{J}_{2,2}^{-1} , \quad (10)$$

which involves the term $\mathbf{J}_{2,2}$ only, which therefore describes propagation of risk across variables.

C. Financial applications: Stress Testing and Risk Allocation

1. Financial applications: Stress Testing

A typical stress test for financial institutions, required by regulatory bodies, consists in forecasting the effect of severe financial and economic shocks on the balance sheet of a financial institution. In this context let's reformulate the previous results by considering \mathbf{X}_1 the set of economic and financial variables that can be shocked and \mathbf{X}_2 the set of the securities held in an institution's portfolio. Assuming that all the changes in the economic and financial variables and in the assets of the portfolio can be modelled as a GMRF, then Eq.8 represents the distribution of the returns of the portfolio (\mathbf{X}_2) conditional on the realization of the economic and financial shocks (\mathbf{X}_1). An approach along similar lines was proposed in [56, 57]. We note that with the LoGo approach we have a sparse relationship between the financial variables and the securities. This makes calibration more robust and it can be insightful to identify mechanisms of impact and vulnerabilities.

2. Risk Allocation

A second application is the calculation of conditional statistics in the presence of linear constraints (see [2]). In this case we indicate with \mathbf{X} a set of p random variables associated with the returns in a portfolio of p assets and with \mathbf{J} the associated sparse inverse covariance matrix. Let $\mathbf{w} \in \mathbb{R}^{p \times 1}$ be the vector of holdings of the portfolio, then $\mathbf{w}^T \cdot \mathbf{X}$ is the return of the portfolio. An important question in portfolio management is to allocate profits and losses to different assets conditional on a given level of profit or loss, which is equivalent to knowing the distribution of returns conditional on a given level of loss $\mathbf{X} | \mathbf{w}^T \cdot \mathbf{X} = \mathbf{L}$. More generally we want to estimate $\mathbf{X} | \mathbf{A} \cdot \mathbf{X} = \mathbf{e}$ where $\mathbf{A} \in \mathbb{R}^{k \times p}$ is generally a low rank k ($k = 1$ in our example) matrix that specifies k hard linear constraints. Using the Lagrange Multipliers method (see [58] for an introduction) the conditional mean is calculated as ([2]):

$$\mathbb{E}(\mathbf{X} | \mathbf{A} \cdot \mathbf{X} = \mathbf{e}) = \mathbf{A} \mathbf{J}^{-1} \left(\mathbf{A} \mathbf{J}^{-1} \mathbf{A}^T \right)^{-1} \mathbf{e} \quad (11)$$

and the conditional covariance is:

$$\mathbf{Cov}(\mathbf{X} | \mathbf{A} \cdot \mathbf{X} = \mathbf{e}) = \mathbf{J}^{-1} - \mathbf{J}^{-1} \mathbf{A}^T \left(\mathbf{A} \mathbf{J}^{-1} \mathbf{A}^T \right)^{-1} \mathbf{A} \mathbf{J}^{-1} \quad (12)$$

In case \mathbf{J} is estimated using decomposable information filtering networks (MST or TMFG) then it can be written as a sum of smaller matrices (as in algorithm 1) involving cliques and separators:

$$\mathbf{J} = \sum_{\mathcal{C} \in \text{Cliques}} \mathbf{J}_{\mathcal{C}} - \sum_{\mathcal{S} \in \text{Separators}} \mathbf{J}_{\mathcal{S}} \quad (13)$$

This decomposition allows for a sparse and potentially parallel evaluation of the matrix products in Eq.s 11 and 12.

This framework can therefore be used to build the Profit/Loss (P/L) distribution of a portfolio, conditionally on a number of explanatory variables, and to allocate the P/L to the different assets conditional on the realization of a given level of profit and loss. The solution is analytical and therefore extremely quick. Besides, given the decomposability of the portfolio, Eq.13 allows to calculate important statistics in parallel, by applying the calculations locally to the cliques and to the separators. For instance, it is a simple exercise to show that the unconditional expected P/L and the unconditional volatility can be calculated in parallel by adding the contributions of the cliques and subtracting the contributions of the separators. In summary LoGo provides the possibility to build a basic risk management framework that allows risk aggregation, allocation, stress testing and scenario analysis in a multivariate Gaussian framework in a quick and potentially parallel fashion.

IV. CONCLUSIONS

We have introduced a methodology, LoGo, that makes use of information filtering networks to produce sparse models that have high likelihood and good predictive power. This method produces high-dimensional sparse inverse covariances by using low-dimensional local inversions only, making the procedure computationally very efficient and little sensitive to the curse of dimensionality. By comparing the results with a state-of-the-art Glasso procedure we obtain, in a fraction of the computation time, equivalent or better results with a sparser and more meaningful network structure. The construction through a sum of local inversion, which is at the basis of LoGo, makes this method very suitable for parallel computing and dynamical adaptation by local, partial updating. We discussed the wide potential applicability of LoGo for sparse inverse covariance estimation, for sparse forecasting models and for financial applications such as stress-testing and risk allocation.

In this paper we presented a simple implementation of the method where a MST or a TMFG chordal planar graph are build in a greedy way by maximising likelihood locally for a linear multivariate model. A natural extension would be to use Akaike Information Criterion [21, 22] instead of likelihood and let a chordal graph to be constructed through local moves without constraining a priori its final topological properties. This would produce simplicial complexes that are clique trees or forests which generalize the MST and TMFG studied in this paper.

The model introduced in this paper is a second-order solution of the maximum entropy problem, resulting in linear, normal multivariate modelling. It is however well known that many real systems follow non-linear probability distributions. Linearity is a severe limitation which can however be overcome by extending LoGo to a much broader class of non-linear models by using the so-called kernel trick [59]. Other generalisations to non-linear transelliptical models [60] can also be implemented. These would be however, the topics of future works.

Acknowledgements

T.A. acknowledges support of the UK Economic and Social Research Council (ESRC) in funding the Systemic Risk Centre (ES/K002309/1). TDM wishes to thank the COST Action TD1210 for partially supporting this work. We acknowledge Bloomberg for providing the data.

-
- [1] S. L. Lauritzen, *Graphical Models* (Oxford:Clarendon, 1996).
 - [2] H. Rue and L. Held, *Gaussian Markov Random Fields: Theory and Applications*, vol. 104 of *Monographs on Statistics and Applied Probability* (Chapman & Hall, London, 2005).
 - [3] T. A. Davis, *Direct methods for sparse linear systems*, vol. 2 (Siam, 2006).
 - [4] C. Wang, N. Komodakis, and N. Paragios, *Comput. Vis. Image Underst.* **117**, 1610 (2013), ISSN 1077-3142.
 - [5] A. Montanari, *Compressed Sensing: Theory and Applications* pp. 394–438 (2012).
 - [6] M. Tumminello, T. Aste, T. Di Matteo, and R. N. Mantegna, *Proceedings of the National Academy of Sciences of the United States of America* **102**, 10421 (2005).
 - [7] T. Aste, W. Shaw, and T. Di Matteo, *New Journal of Physics* **12**, 085009 (2010).
 - [8] F. Pozzi, T. Di Matteo, and T. Aste, *Scientific Reports* **3**, 1665 (2013).
 - [9] N. Musmeci, T. Aste, and T. Di Matteo, *PLoS ONE* **10**, e0116201 (2015).
 - [10] N. Musmeci, T. Aste, and T. Di Matteo, *Network Theory in Finance* **1**, 77 (2015).
 - [11] X. Wu, Y. Ye, K. R. Subramanian, and L. Zhang, in *BIOKDD* (2003), vol. 3, pp. 63–69.
 - [12] J. Schäfer and K. Strimmer, *Bioinformatics* **21**, 754 (2005).

- [13] T. R. Lezon, J. R. Banavar, M. Cieplak, A. Maritan, and N. V. Fedoroff, *Proceedings of the National Academy of Sciences* **103**, 19033 (2006), <http://www.pnas.org/content/103/50/19033.full.pdf+html>.
- [14] E. Schneidman, M. J. Berry, R. Segev, and W. Bialek, *Nature* **440**, 1007 (2006).
- [15] T. Zerenner, P. Friederichs, K. Lehnertz, and A. Hense, *Chaos: An Interdisciplinary Journal of Nonlinear Science* **24**, 023103 (2014).
- [16] I. Ebert-Uphoff and Y. Deng, *Geophysical Research Letters* **39**, 1 (2012).
- [17] M. Haran, *Handbook of Markov Chain Monte Carlo* pp. 449–478 (2011).
- [18] D. T. Hristopulos and S. N. Elogne, *Signal Processing, IEEE Transactions on* **57**, 3475 (2009).
- [19] D. T. Hristopulos, *SIAM Journal on Scientific Computing* **24**, 2125 (2003).
- [20] Y. Zhou, arXiv preprint arXiv:1111.6925 (2011).
- [21] H. Akaike, *Automatic Control, IEEE Transactions on* **19**, 716 (1974).
- [22] H. Akaike, in *Selected Papers of Hirotugu Akaike* (Springer, 1998), pp. 199–213.
- [23] S. Kullback and R. A. Leibler, *The annals of mathematical statistics* **22**, 79 (1951).
- [24] G. Schwarz et al., *The annals of statistics* **6**, 461 (1978).
- [25] J. Rissanen, *Automatica* **14**, 465 (1978).
- [26] F. Petitjean, G. Webb, A. E. Nicholson, et al., in *Data Mining (ICDM), 2013 IEEE 13th International Conference on* (IEEE, 2013), pp. 597–606.
- [27] P. Giudici, Green, and P.J, *Biometrika* **86**, 785 (1999).
- [28] A. Deshpande, M. Garofalakis, and M. I. Jordan, in *Proceedings of the Seventeenth conference on Uncertainty in artificial intelligence* (Morgan Kaufmann Publishers Inc., 2001), pp. 128–135.
- [29] F. R. Bach and M. I. Jordan, in *Advances in Neural Information Processing Systems* (2001), pp. 569–576.
- [30] N. Srebro, in *Proceedings of the Seventeenth conference on Uncertainty in artificial intelligence* (Morgan Kaufmann Publishers Inc., 2001), pp. 504–511.
- [31] A. Checheta and C. Guestrin, in *Advances in Neural Information Processing Systems* (2008), pp. 273–280.
- [32] A. d’Aspremont, O. Banerjee, and L. El Ghaoui, *SIAM Journal on Matrix Analysis and Applications* **30**, 56 (2008).
- [33] O. Banerjee, L. El Ghaoui, and A. d’Aspremont, *The Journal of Machine Learning Research* **9**, 485 (2008).
- [34] O. Banerjee, L. E. Ghaoui, A. d’Aspremont, and G. Natsoulis, in *Proceedings of the 23rd international conference on Machine learning* (ACM, 2006), pp. 89–96.
- [35] R. Tibshirani, *Journal of the Royal Statistical Society, Series B* **58**, 267 (1996).
- [36] H. Zou and T. Hastie, *Journal of the Royal Statistical Society: Series B (Statistical Methodology)* **67**, 301 (2005).
- [37] N. Meinshausen and P. Bühlmann, *Annals of Statistics* **34**, 1436 (2006).
- [38] O. Banerjee, L. El Ghaoui, and A. d’Aspremont, *J. Mach. Learn. Res.* **9**, 485 (2008), ISSN 1532-4435.
- [39] P. Ravikumar, M. J. Wainwright, G. Raskutti, and B. Yu, *Electronic Journal of Statistics* **5**, 935 (2011).
- [40] C. Hsieh, I. S. Dhillon, P. K. Ravikumar, and M. A. Sustik, in *Advances in Neural Information Processing Systems 24*, edited by J. Shawe-Taylor, R. Zemel, P. Bartlett, F. Pereira, and K. Weinberger (Curran Associates, Inc., 2011), pp. 2330–2338.
- [41] F. Oztoprak, J. Nocedal, S. Rennie, and P. A. Olsen, in *Advances in Neural Information Processing Systems 25*, edited by P. Bartlett, F. Pereira, C. Burges, L. Bottou, and K. Weinberger (2012), pp. 755–763.
- [42] J. Friedman, T. Hastie, and R. Tibshirani, *Biostatistics (Oxford, England)* **9**, 432 (2008).
- [43] R. N. Mantegna, *The European Physical Journal B - Condensed Matter and Complex Systems* **11**, 193 (1999).
- [44] T. Aste and T. Di Matteo, *Physica A* **370**, 156 (2006).
- [45] W.-M. Song, T. Di Matteo, and T. Aste, *PLoS ONE* **7**, e31929 (2012).
- [46] G. P. Massara, T. Di Matteo, and T. Aste, *Journal of Complex Networks* (2016); arXiv preprint arXiv:1505.02445.
- [47] E. T. Jaynes, *The Physical Review* **106**, 620 (1957).
- [48] E. T. Jaynes, *The Physical Review* **108**, 171 (1957).
- [49] H. Hotelling, *Journal of the Royal Statistical Society. Series B (Methodological)* **15**, 193 (1953), ISSN 00359246.
- [50] A. P. Dempster, *Biometrics* **28**, 157 (1972).
- [51] R. Diestel, *Graph Theory*, vol. 173 of *Graduate Texts in Mathematics* (Springer, Heidelberg, 2010).
- [52] P. G. Hoel et al., *Introduction to mathematical statistics*. (1954).
- [53] J. B. Kruskal Jr., *Proceedings of the American Mathematical Society* **7**, 48 (1956).
- [54] R. Prim, *Bell System Technical Journal, The* **36**, 1389 (1957), ISSN 0005-8580.
- [55] F. Pedregosa, G. Varoquaux, A. Gramfort, V. Michel, B. Thirion, O. Grisel, M. Blondel, P. Prettenhofer, R. Weiss, V. Dubourg, et al., *Journal of Machine Learning Research* **12**, 2825 (2011).
- [56] R. Rebonato, *Coherent stress testing* (2010).
- [57] A. Denev, *Probabilistic Graphical Models: A New Way of Thinking in Financial Modelling* (Risk Books, 2015).
- [58] G. Strang, *Introduction to Applied Mathematics* (Wellesley-Cambridge Press, 1986), ISBN 9780961408800.
- [59] J. Shawe-Taylor and N. Cristianini, *Kernel methods for pattern analysis* (Cambridge university press, 2004).
- [60] H. Liu, F. Han, and C.-h. Zhang, in *Advances in Neural Information Processing Systems* (2012), pp. 809–817.